

AD-A014 425

**CROSS-SPECTRAL PROPERTIES OF SOME COMMON WAVEFORMS
IN THE PRESENCE OF UNCORRELATED NOISE**

Alan E. Markowitz

**Naval Underwater Systems Center
New London, Connecticut**

6 August 1975

DISTRIBUTED BY:

NTIS

**National Technical Information Service
U. S. DEPARTMENT OF COMMERCE**

259083

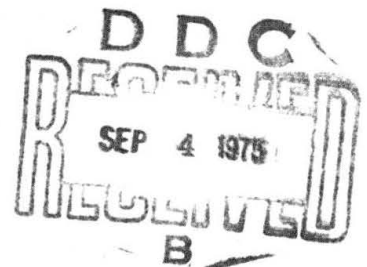
NUSC Technical Report 4947

Cross-Spectral Properties of Some Common Waveforms in the Presence of Uncorrelated Noise

ALAN E. MARKOWITZ
Submarine Sonar Department



6 August 1975



NAVAL UNDERWATER SYSTEMS CENTER

New London Laboratory

Approved for public release; distribution unlimited.

Reproduced by
NATIONAL TECHNICAL
INFORMATION SERVICE
U.S. Department of Commerce
Springfield, VA. 22151

ADA014425

PREFACE

This study was performed under NUSC Project No. A-134-03, "Towed Array Noise Modeling," Principal Investigator, A. E. Markowitz (Code SA14), and Navy Subproject and Task No. SF 11 121 702-15122, Program Manager, C. C. Walker, Naval Sea Systems Command (Code SEA 06H1-2).

The Technical Reviewer for this report was G. C. Carter (Code TF).

The author is grateful to Dr. A. H. Nuttall (NUSC) for his suggestion of the approach to be taken in the appendix and for pointing out the significance of the distribution of the random initial phases associated with each of the wave components. Also, the author is indebted to Dr. R. T. Menton (NUSC) for his helpful suggestions, technical criticism, and encouragement.

REVIEWED AND APPROVED: 6 August 1975

ACCESSION for	
NTIS	White Section <input checked="" type="checkbox"/>
D.C.	Buff Section <input type="checkbox"/>
USA (NUSC)	<input type="checkbox"/>
JUSTIFICATION	
BY	
DISTRIBUTION/AVAILABILITY CODES	
Dist.	Avail. and/or SPECIAL
A	

W.A. McChally
for C. A. Spero, Jr.
Director, Systems Development

The author of this report is located at the New London Laboratory, Naval Underwater Systems Center, New London, Connecticut 06320.

UNCLASSIFIED

SECURITY CLASSIFICATION OF THIS PAGE (When Data Entered)

REPORT DOCUMENTATION PAGE		READ INSTRUCTIONS BEFORE COMPLETING FORM
1. REPORT NUMBER TR 4947	2. GOVT ACCESSION NO.	3. RECIPIENT'S CATALOG NUMBER
4. TITLE (and Subtitle) CROSS-SPECTRAL PROPERTIES OF SOME COMMON WAVEFORMS IN THE PRESENCE OF UNCORRELATED NOISE		5. TYPE OF REPORT & PERIOD COVERED
		6. PERFORMING ORG. REPORT NUMBER
7. AUTHOR(s) Alan E. Markowitz		8. CONTRACT OR GRANT NUMBER(s)
9. PERFORMING ORGANIZATION NAME AND ADDRESS Naval Underwater Systems Center New London Laboratory New London, Connecticut 06320		10. PROGRAM ELEMENT, PROJECT, TASK AREA & WORK UNIT NUMBERS A-134-03 SF 11 121 702-15122
11. CONTROLLING OFFICE NAME AND ADDRESS Naval Sea Systems Command (SEA 06H1-2) Washington, DC 20360		12. REPORT DATE 6 August 1975
		13. NUMBER OF PAGES 34
14. MONITORING AGENCY NAME & ADDRESS (if different from Controlling Office)		15. SECURITY CLASS. (of this report) UNCLASSIFIED
		15a. DECLASSIFICATION/DOWNGRADING SCHEDULE
16. DISTRIBUTION STATEMENT (of this Report) Approved for public release; distribution unlimited.		
17. DISTRIBUTION STATEMENT (of the abstract entered in Block 20, if different from Report)		
18. SUPPLEMENTARY NOTES		
19. KEY WORDS (Continue on reverse side if necessary and identify by block number) Cross-spectral properties Traveling wave components Magnitude coherence Uncorrelated noise Phase Waveforms Self-Noise		
20. ABSTRACT (Continue on reverse side if necessary and identify by block number) The magnitude coherence and phase for a number of common waveforms in the presence of uncorrelated noise is derived mathematically and presented graphically. Discussion is limited to waveforms resulting from the combination of no more than two traveling waves. The effects of the relative magnitude of the traveling wave components, as well as the uncorrelated noise, are seen. The effect of wave speed is also noted. Finally, the periodicity with respect to frequency, observed in the resultant plots, is shown to be significant and is a reflection of the relative wave speeds. A table		

UNCLASSIFIED

SECURITY CLASSIFICATION OF THIS PAGE(When Data Entered)

20. Cont'd.

summarizing the results is also presented.

UNCLASSIFIED

SECURITY CLASSIFICATION OF THIS PAGE(When Data Entered)

TABLE OF CONTENTS

	Page
LIST OF TABLES	11
LIST OF ILLUSTRATIONS	11
INTRODUCTION	1
THEORETICAL BACKGROUND	1
RESULTS	4
General	4
Specific Cases	5
ADDITIONAL COMMENTS	13
APPENDIX--DERIVATION OF MAGNITUDE COHERENCE AND PHASE FOR TWO TRAVELING WAVES IN THE PRESENCE OF UNCORRELATED NOISE	23
LIST OF REFERENCES	29

LIST OF TABLES

Table	Page
1 Summary of Results	22

LIST OF ILLUSTRATIONS

Figure	Page
1 Model for Single Traveling Wave Plus Uncorrelated Noise . .	1
2 Model for Two Traveling Waves Plus Uncorrelated Noise . . .	2
3 $ \gamma_{12} $ for Single Traveling Wave Plus Uncorrelated Noise. . .	6
4 ϕ for Single Traveling Wave	6
5 ϕ for Classical Standing Wave	8
6 $ \gamma_{12} $ for Standing Wave (for $2X/(2X + N) = 0.6$).	8
7 $ \gamma_{12} $ for Standing Wave (for $2X/(2X + N) = 0.8$)	8
8 $ \gamma_{12} $ for Two Waves With $\phi_y = -\phi_x$; Case 1, Zero Noise . . .	9
9 $ \gamma_{12} $ for Two Waves With $\phi_y = -\phi_x$; Case 2, $N = 2/3 (X + Y)$.	9
10 $ \gamma_{12} $ for Two Waves With $\phi_y = -\phi_x$; Case 3, High Noise . . .	9
11 ϕ for Two Waves With $\phi_y = -\phi_x$	10
12 $ \gamma_{12} $ for Two Waves With $\phi_y = -\phi_x$; Maxima, Minima, and Mean.	11
13 $ \gamma_{12} $ for Two Waves With $\phi_y = -\phi_x$; Effect of Relative Wave Magnitudes	11
14 ϕ for Two Waves With $\phi_y = -\phi_x$; Effect of Relative Wave Magnitudes	11
15 ϕ for Equal Magnitude Waves Traveling in Same Direction; Effect of ϕ_y/ϕ_x	12
16 ϕ for Unequal Magnitude Waves Traveling in Same Direction; Effect of X/Y With $\phi_y/\phi_x = 0.1$	14
17 ϕ for Unequal Magnitude Waves Traveling in Same Direction; Effect of X/Y With $\phi_y/\phi_x = 0.5$	15
18 ϕ for Unequal Magnitude Waves Traveling in Same Direction; Effect of X/Y With $\phi_y/\phi_x = 2$	16

LIST OF ILLUSTRATIONS (Cont'd)

Figure		Page
19	ϕ for Unequal Magnitude Waves Traveling in Same Direction; Effect of X/Y With $\phi_y/\phi_x = 3$	17
20	ϕ for Unequal Magnitude Waves Traveling in Opposite Directions; Effect of X/Y With $\phi_y/\phi_x = -0.1$	18
21	ϕ for Unequal Magnitude Waves Traveling in Opposite Directions; Effect of X/Y With $\phi_y/\phi_x = -2$	19
22	Resolving an Ambiguity	21

CROSS-SPECTRAL PROPERTIES OF SOME COMMON WAVEFORMS IN THE PRESENCE OF UNCORRELATED NOISE

INTRODUCTION

An extensive amount of data analysis had been performed in 1974 to determine towed array self-noise mechanisms.^{1,2,3} Reduction of the data, with particular emphasis placed on determining the magnitude coherence and phase, yielded the cross-spectral properties. Since magnitude coherence can be a measure of signal-to-noise ratio⁴ and in conjunction with the phase is a measure of wave speed, it was possible to determine some of the dominant self-noise mechanisms. Interpretation of the data, however, is not always clear cut. In the presence of uncorrelated background noise, various mechanisms can combine in many different ways to produce complicated results. To achieve a better understanding of the self-noise data, it was found useful to investigate the cross-spectral properties of some common waveforms in the presence of uncorrelated noise. It is the purpose of this report to present the results of this investigation, with the hope that it will prove useful to others analyzing these types of data.

THEORETICAL BACKGROUND

This section provides the theoretical background for determining magnitude coherence and phase. For a single traveling wave in the presence of uncorrelated noise, Carter⁴ showed that

$$\left| \gamma_{12}(f) \right| = \frac{X(f)}{X(f) + N(f)} \quad (1)$$

based on the model in figure 1, where $\left| \gamma_{12}(f) \right|$ is the magnitude coherence between observation points 1 and 2. Uncorrelated noise sources $n_1(t)$ and $n_2(t)$ have the respective autospectra $N_1(f)$ and $N_2(f)$, where $N_1(f) = N_2(f) = N(f)$. $X(f)$ is the autospectrum of $x(t)$, which is 100 percent coherent, since it is the same at both observation points. (A computer run experiment using actual at-sea data verified equation (1) and is further discussed in a NUSC memorandum.²)

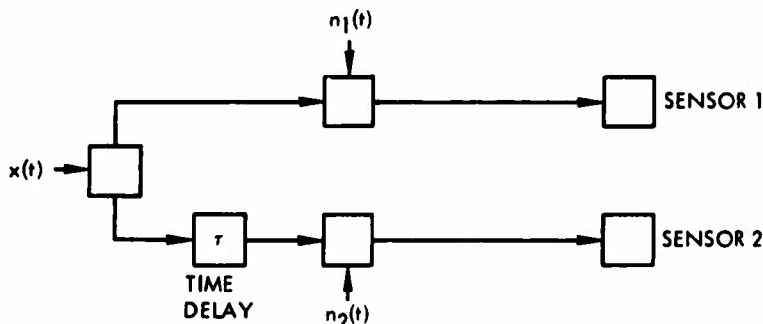


Figure 1. Model for Single Traveling Wave
Plus Uncorrelated Noise

For two independent traveling waves in the presence of uncorrelated noise, Gardner⁵ has shown that

$$\gamma_{12}(f) = \frac{\Gamma_x(f) [X_{11}(f) X_{22}(f)]^{1/2} e^{i\theta_x(f)} + \Gamma_y(f) [Y_{11}(f) Y_{22}(f)]^{1/2} e^{i\theta_y(f)}}{\left\{ [X_{11}(f) + Y_{11}(f)] [X_{22}(f) + Y_{22}(f)] \right\}^{1/2}} \quad (2)$$

where $X_{11}(f)$, $X_{22}(f)$, $Y_{11}(f)$, and $Y_{22}(f)$ are the autospectra for the two independent signals $x(t)$ and $y(t)$ at observation points 1 and 2. Here uncorrelated noise is included as part of the signal. The cross-spectral densities are $\Gamma_x(f) [X_{11}(f) X_{22}(f)]^{1/2} e^{i\theta_x(f)}$ and $\Gamma_y(f) [Y_{11}(f) Y_{22}(f)]^{1/2} e^{i\theta_y(f)}$ (i.e., $X_{12}(f)$ and $Y_{12}(f)$, respectively) and the phases are $\theta_x(f)$ and $\theta_y(f)$. Equation (2) can be written as

$$\gamma_{12}(f) = \frac{X(f) e^{i\theta_x(f)} + Y(f) e^{i\theta_y(f)}}{X(f) + Y(f) + N(f)} \quad (3)$$

as shown by Markowitz⁶, for the model in figure 2.

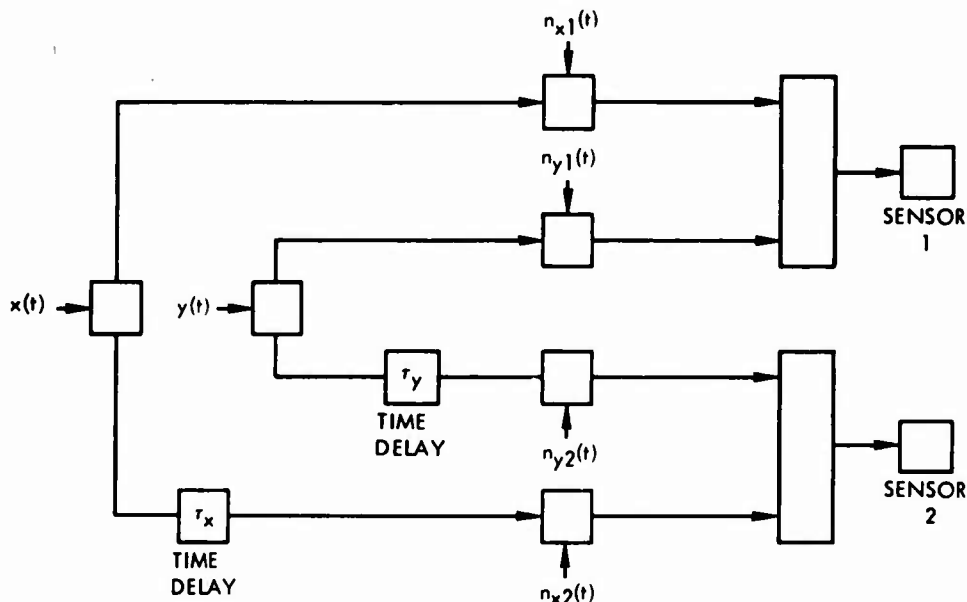


Figure 2. Model for Two Traveling Waves Plus Uncorrelated Noise

In the figure $n_{x1}(t)$, $n_{x2}(t)$, $n_{y1}(t)$, and $n_{y2}(t)$ are uncorrelated noise sources with autospectra $N_{x1}(f) = N_{x2}(f) = N_x(f)$ and $N_{y1}(f) = N_{y2}(f) = N_y(f)$. The signals $x(t)$ and $y(t)$ are each 100 percent coherent in the model and have the respective autospectra $X(f)$ and $Y(f)$. Also, $X_{11}(f) = X_{22}(f) = X(f) + N_x(f)$, $Y_{11}(f) = Y_{22}(f) = Y(f) + N_y(f)$, and $N_x(f) + N_y(f) = N(f)$. We note that $\theta_x = \omega d/c_x$ and $\theta_y = (\omega d/c_y)$, where d is the spatial separation between sensors 1 and 2 and c_x , c_y are the respective x and y velocities.

A derivation of equation (3) is given in the appendix. The important assumptions made there are that (1) waves are nondispersive; (2) no attenuation between observation points 1 and 2; (3) $x(t)$ and $y(t)$ signals in equation (3) are independent and, therefore, uncorrelated with respect to each other; and (4) the estimate of the initial phases associated with each wave are uniformly distributed from $-\pi$ to $+\pi$.

The magnitude coherence and phase obtained from equation (3) are

$$|\gamma_{12}(f)| = \frac{\left\{ X(f)^2 + Y(f)^2 + 2X(f)Y(f) \cos [\theta_x(f) - \theta_y(f)] \right\}^{1/2}}{X(f) + Y(f) + N(f)} \quad (4)$$

and

$$\theta = \tan^{-1} \left\{ \frac{X(f) \sin \theta_x(f) + Y(f) \sin \theta_y(f)}{X(f) \cos \theta_x(f) + Y(f) \cos \theta_y(f)} \right\}. \quad (5)$$

The significance of the third assumption, regarding the statistical independence of $x(t)$ and $y(t)$, can readily be seen in the special case of standing waves. Consider $x(t)$ and $y(t)$ to be of unity magnitude and traveling in opposite directions at frequency $\omega_0 = 2\pi f_0$ to form the standing wave $S_1 = \cos k_0 x_1 e^{i\omega_0 t}$ at observation point 1 and $S_2 = \cos k_0 x_2 e^{i\omega_0 t}$ at observation point 2. One can then form the cross correlation to obtain

$$\begin{aligned} R_{12}(\tau) &= \frac{1}{T} \int_{-T/2}^{T/2} \cos k_0 x_1 \cos k_0 x_2 e^{-i2\pi f_0 t} e^{i2\pi f_0 (t+\tau)} dt \\ \lim_{T \rightarrow \infty} &= \cos k_0 x_1 \cos k_0 x_2 e^{i2\pi f_0 \tau}. \end{aligned}$$

The cross-spectral density becomes

$$\begin{aligned} G_{12}(f) &= \int_{-\infty}^{\infty} \cos k_0 x_1 \cos k_0 x_2 e^{i2\pi f_0 \tau} e^{i2\pi f \tau} d\tau \\ &= \cos k_0 x_1 \cos k_0 x_2 2\pi \delta(2\pi f - 2\pi f_0) \\ &= \cos k_0 x_1 \cos k_0 x_2 \delta(f - f_0). \end{aligned}$$

Normalizing via $G_{11}(f)$ and $G_{22}(f)$ yields

$$|\gamma_{12}(f)| = \left| \frac{\cos(\omega_0 x_1/c) \cos(\omega_0 x_2/c)}{|\cos(\omega_0 x_1/c)| |\cos(\omega_0 x_2/c)|} \right| = 1 \quad (6)$$

$$\theta = \left. \begin{array}{l} 0 \\ \pi \end{array} \right\} \begin{array}{l} \text{in phase} \\ \text{out of phase} \end{array}, \quad (7)$$

where c is the wave speed (ω_0/k_0). (Uncorrelated noise sources are ignored temporarily, since, for the purpose of demonstrating the significance of the third

assumption, they represent an unnecessary complication.) These results (equations (6) and (7)) differ substantially from the previous results (equations (4) and (5)). For a standing wave, equations (4) and (5) show, respectively, $|Y_{12}(f)|$ to be periodic in f and θ to be spatially homogeneous, whereas equations (6) and (7) show, respectively, $|Y_{12}(f)| = 1$ and θ to be nonhomogeneous, depending upon actual values of x_1 and x_2 . The difference lies in the fact that in equations (6) and (7) the x and y traveling wave components of the standing wave are not statistically independent, but in equations (4) and (5) they are. This difference is shown mathematically in the appendix, where the estimate of the cross-spectral properties of the combined signals are obtained via ensemble averaging. In each computation of the cross-spectral density, an initial phase is associated with each traveling wave. When the two waves are statistically independent, this initial phase is taken to be random, with a uniform distribution from $-\pi$ to π . When the ensemble average is formed, various cross-product terms drop out because of the random phase relationship and, thereby, equations (4) and (5) are obtained. In equations (6) and (7), the initial phase is assumed to be zero, resulting in a deterministic phase relationship, namely zero; consequently the results are different.

RESULTS

GENERAL

This section is essentially a graphic representation of equations (4) and (5) for variations of the pertinent parameters. These parameters are relative wave speed determined by θ_x and θ_y , relative magnitude determined by $X(f)$ and $Y(f)$, and relative uncorrelated noise determined by $N(f)$. For simplicity, the frequency dependence of $X(f)$, $Y(f)$, and $N(f)$ is neglected; i.e., the autospectra of $x(t)$, $y(t)$, and $n(t)$ are constant with respect to frequency, and equations (4) and (5) become, respectively,

$$|Y_{12}(f)| = \frac{[X^2 + Y^2 + 2XY \cos(\theta_x - \theta_y)]^{1/2}}{X + Y + N} \quad (8)$$

and

$$\theta = \tan^{-1} \frac{(X \sin \theta_x + Y \sin \theta_y)}{(X \cos \theta_x + Y \cos \theta_y)}, \quad (9)$$

where $X(f)$, $Y(f)$, and $N(f)$ are now simply written X , Y , and N .

Results are presented as a function of θ_x for various values of θ_y/θ_x . In actual practice, $|Y_{12}|$ and θ are obtained as functions of frequency. The conversion is readily made since

$$\theta_x = 2\pi fd/c_x \text{ and } \theta_y = 2\pi fd/c_y, \quad (10,11)$$

where d is the spatial separation between sensors 1 and 2, and c_x and c_y are the respective wave velocities for $x(t)$ and $y(t)$.

In general, the coherence function will reflect a periodicity with respect to frequency because of the term $[2XY \cos 2\pi f(\frac{d}{c_x} - \frac{d}{c_y})]$. In fact, a single period

with respect to frequency, denoted Δf , is exactly $c_x c_y / d(c_y - c_x)$:

$$\Delta f = c_x c_y / d(c_y - c_x). \quad (12)$$

This periodicity is very important in determining self-noise mechanisms, since it is a reflection of wave speed, which is associated with the self-noise mechanisms (i.e., 5000 ft/sec is associated with acoustic waves). Of course, the fact that we are dealing with two speeds can present complicated results. When only one wave speed exists (i.e., $c_x = c_y$ or $Y = 0$) $\Delta f \rightarrow \infty$ and $|\gamma_{12}|$ is a constant.

We note that the phase is independent of N . However, from a computational point of view, uncorrelated noise is important in actual practice, since the variance for the computed estimate of the phase depends on the coherence and, therefore, on N .

SPECIFIC CASES

Discussion here is limited to waveforms resulting from the combination of no more than two traveling waves. Four waveforms are investigated:

1. Single Traveling Wave Plus Uncorrelated Noise

Equations (8) and (9), respectively, reduce to

$$|\gamma_{12}(f)| = \frac{X}{X + N} \text{ and } \theta = \theta_x \quad (13,14)$$

(see figures 3 and 4). We note that $|\gamma_{12}|$ is constant and this indicates that only one wave speed exists, hence only one self-noise mechanism. This wave speed is $c = 2\pi d / (\theta/f)$, where (θ/f) is the slope of the phase plot.

2. Waves With $\theta_y = -\theta_x$ Plus Uncorrelated Noise

Equations (8) and (9) reduce to

$$|\gamma_{12}(f)| = \frac{(X^2 + Y^2 + 2XY \cos 2\theta_x)^{1/2}}{X + Y + N} \quad (15)$$

and

$$\theta = \tan^{-1} \left[\frac{(X - Y) \tan \theta_x}{(X + Y)} \right]. \quad (16)$$

The magnitude coherence is periodic in θ_x , with a period of π radians corresponding to $\Delta f = c_x / 2d$. The speed of the traveling components of waves with $\theta_y = -\theta_x$ is, therefore, $c = 2d\Delta f$.

2a. Equal Magnitude Traveling Wave Components (Classical Standing Wave)

Equations (15) and (16) become, respectively,

$$|\gamma_{12}(f)| = \frac{X}{2X + N} (2 + 2 \cos 2\theta_x)^{1/2} = \frac{2X}{2X + N} \left| \cos \theta_x \right| \quad (17)$$

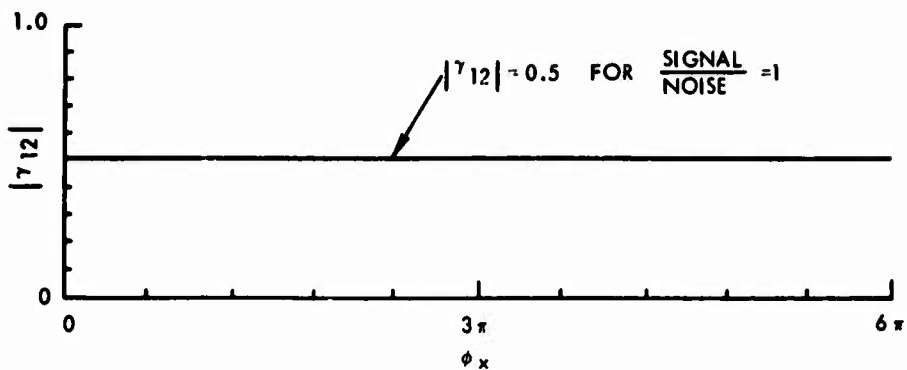


Figure 3. $|\gamma_{12}|$ for Single Traveling Wave Plus Uncorrelated Noise

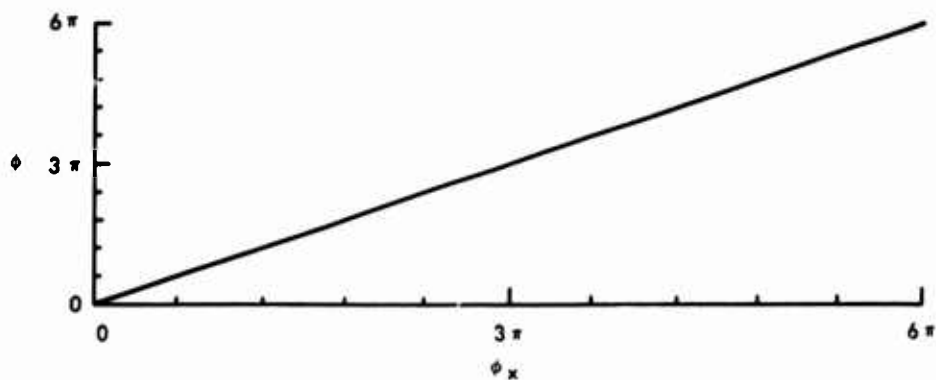


Figure 4. ϕ for Single Traveling Wave

and

$$\theta = \begin{cases} 0 & 0 \leq \theta_x < \pi/2, \pi < \theta_x < 3\pi/2 \text{ (i.e., } \tan \theta_x \text{ is positive)} \\ \pi & \pi/2 < \theta_x \leq \pi, 3\pi/2 < \theta_x < 2\pi \text{ (i.e., } \tan \theta_x \text{ is negative)} \end{cases} \quad (18)$$

The essential characteristics of the classical standing wave, shown in figures 5-7, are as follows:

- Figure 5 shows the step function characteristic of the phase where θ contains jumps of π radians. This is superimposed over the traveling wave component for reference.
- Figure 6 shows the periodic characteristic of the standing wave for $2X/(2X + N) = 0.6$. The nominal values chosen were $X = Y = 3$ and $N = 4$. We note that for equal magnitude components the minima occur at $|\gamma_{12}| = 0$ and the maxima at $2X/(2X + N)$. The frequency period is $\Delta f = c_x/2d$ or, with respect to θ_x , it is π .
- Figure 7 shows that as the noise (N) is reduced, the peak increases to the new value of $2X/(2X + N)$, which, in this case, is 0.8. The nominal values chosen were $X = Y = 2$ and $N = 1$.

2b. Unequal Magnitude Traveling Wave Components

For $Y = 2X$, as an example, equations (15) and (16) become, respectively,

$$|\gamma_{12}(f)| = \frac{X(5 + 4 \cos 2\theta_x)^{1/2}}{3X + N} = \frac{X}{3X + N} (1 + 8 \cos^2 \theta_x)^{1/2}$$

and

$$\theta = \tan^{-1} (1/3 \tan \theta_x).$$

These results are shown in figures 8-10. As for all waves with $\theta_y = -\theta_x$, the periodicity of $|\gamma_{12}|$ with respect to θ_x is π .

The minima are no longer zero, as previously observed for $X = Y$, but depend on the noise (N). The effect of N is to control the minimum points, peak points, and peak-to-valley excursions. These values decrease as N increases.

Characteristics of the phase plot are seen in figure 11 to be between the standing wave step function ($X = Y$) case and the straight line single traveling wave case, which again is shown for reference in the figure.

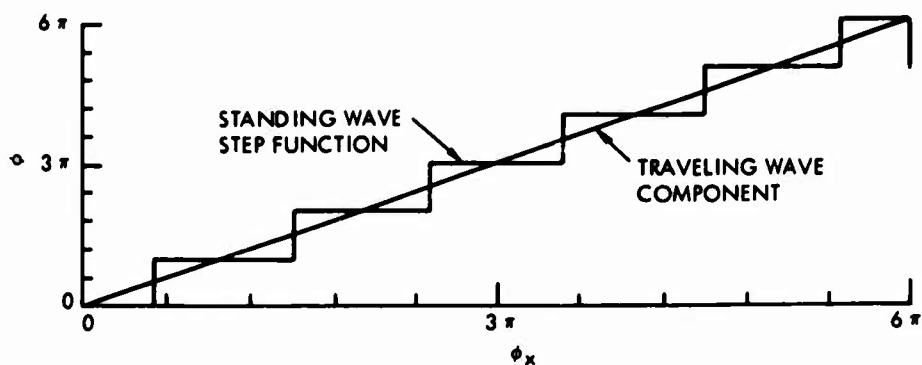


Figure 5. ϕ for Classical Standing Wave

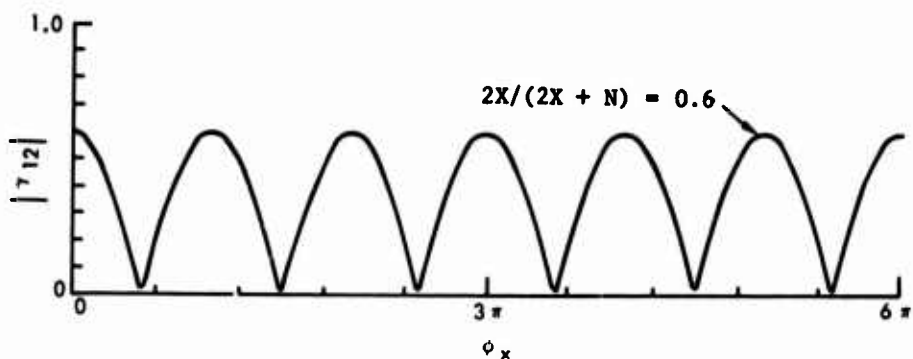


Figure 6. $|\gamma_{12}|$ for Standing Wave (for $2X/(2X + N) = 0.6$)

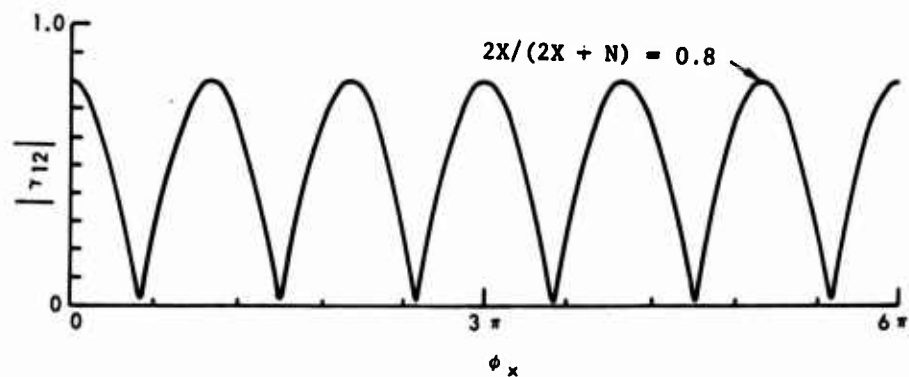


Figure 7. $|\gamma_{12}|$ for Standing Wave (for $2X/(2X + N) = 0.8$)

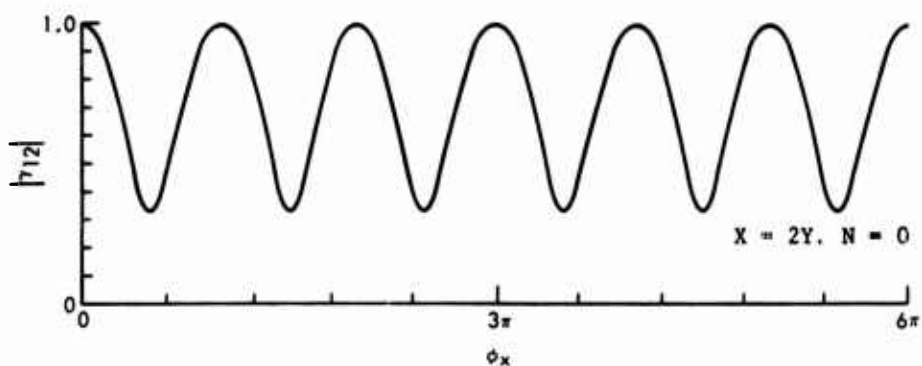


Figure 8. $|\gamma_{12}|$ for Two Waves With $\phi_y = -\phi_x$; Case 1, Zero Noise

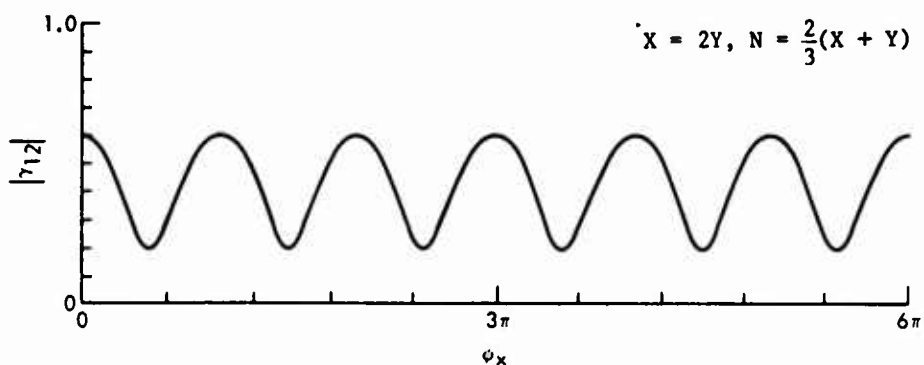


Figure 9. $|\gamma_{12}|$ for Two Waves With $\phi_y = -\phi_x$; Case 2, $N = \frac{2}{3}(X + Y)$

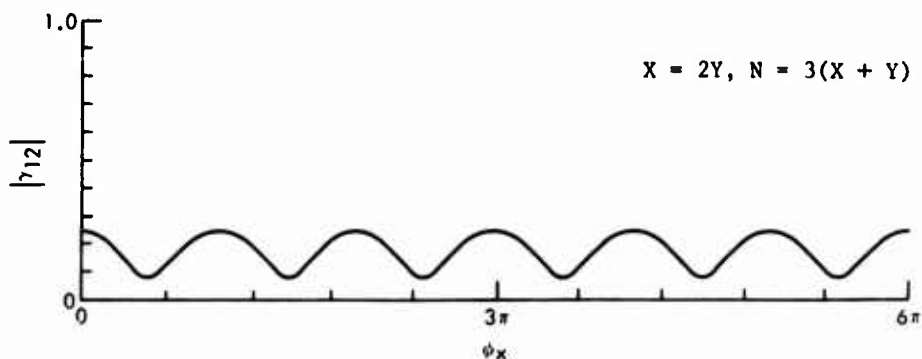


Figure 10. $|\gamma_{12}|$ for Two Waves With $\phi_y = -\phi_x$; Case 3, High Noise

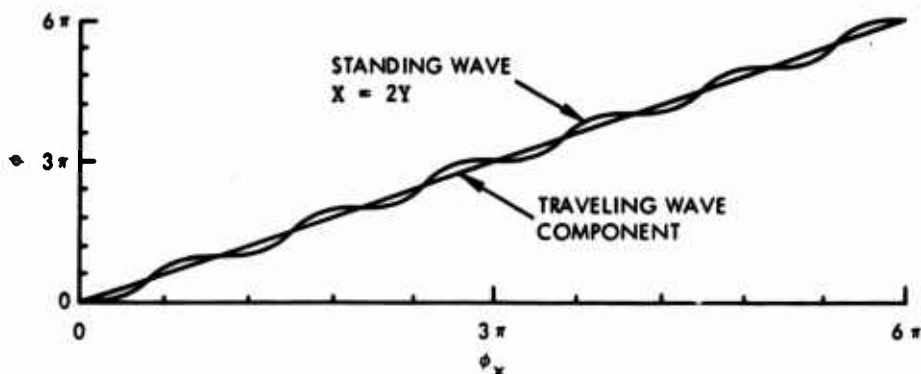


Figure 11. ϕ for Two Waves With $\phi_y = -\phi_x$

We can now generalize. For waves with $\phi_y = -\phi_x$, the range of $|\gamma_{12}|$ is

$$\frac{X - Y}{X + Y + N} \leq |\gamma_{12}| \leq \frac{X + Y}{X + Y + N} \quad (19)$$

and if we assume by convention $X > Y$, then the mean value of $|\gamma_{12}|$ will be

$$|\gamma_{12}| \text{ mean} = \frac{X}{X + Y + N} \quad X > Y, \quad (20)$$

with an excursion of $\pm Y/(X + Y + N)$, as shown in figure 12.

Therefore, as $Y \rightarrow X$, for a given N , the minima approach zero, the peak-to-valley excursion is maximized, and $|\gamma_{12}|$ mean is reduced. For $X \gg Y$, the results approach the single traveling wave case. This is seen in figure 13 for $X = 2Y$, $X = 5Y$, $X = 11Y$, and $N = 2/3(X + Y)$. Thus, as (X/Y) increases, $|\gamma_{12}|$ becomes more nearly constant.

The generalization pertaining to ϕ is simply that as $X/Y \rightarrow 1$ the characteristic step function, seen in figure 5, is observed, and as $X \gg Y$ the results approach the single traveling wave case shown in figure 4. Figure 11 presents an "in between" case, where $X = 2Y$. Finally, figure 14 compares $X = 5Y$ with $X = 2Y$, where the former case is already approaching the straight line condition.

3. Two Waves Traveling in Same Direction

From equation (8) we note that the magnitude coherence will have a periodicity in f dependent upon $(\phi_x - \phi_y)$ and is indistinguishable from other waveforms with similar characteristics. For example, a wave with $\phi_y = -\phi_x$ having traveling wave components X_{sw} and Y_{sw} and a phase velocity of ϕ_{xsw} is compared with the sum of two waves, X_{tw} and Y_{tw} , traveling in the same direction with phases ϕ_{xtw} and ϕ_{ytw} . Their magnitude coherences are indistinguishable if

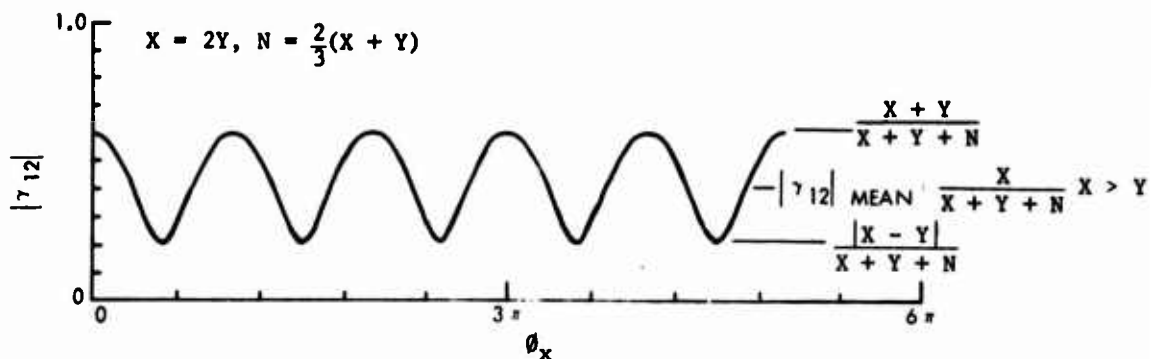


Figure 12. $|\gamma_{12}|$ for Two Waves With $\theta_y = -\theta_x$; Maxima, Minima, and Mean

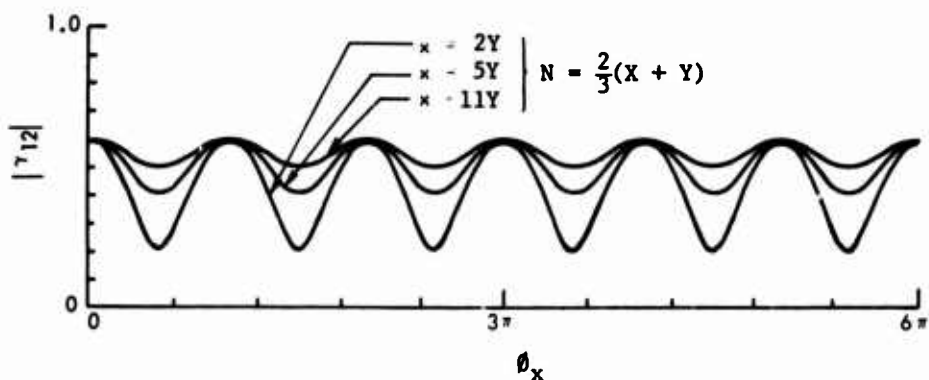


Figure 13. $|\gamma_{12}|$ for Two Waves With $\theta_y = -\theta_x$; Effect of Relative Wave Magnitudes

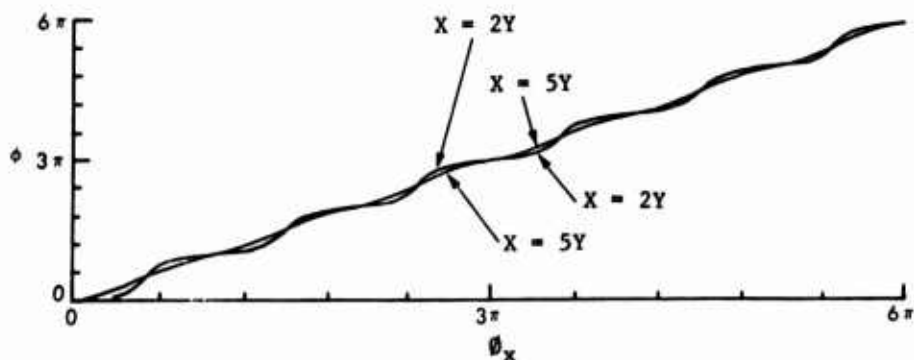


Figure 14. θ for Two Waves With $\theta_y = -\theta_x$; Effect of Relative Wave Magnitudes

$X_{sw} = X_{tw}$, $Y_{sw} = Y_{tw}$, and $2\theta_{xsw} = (\theta_{xtw} - \theta_{ytw})$. This situation is discussed further on p. 13.

3a. Equal Magnitude Components

For equal magnitude traveling waves, equation (9) becomes

$$\theta = \tan^{-1} \left[\frac{\sin \theta_x + \sin \theta_y}{\cos \theta_x + \cos \theta_y} \right] = \frac{\theta_x + \theta_y}{2} \quad (21)$$

Thereby, θ becomes a linear function of θ_x for given values of (θ_y/θ_x) and is shown in figure 15.

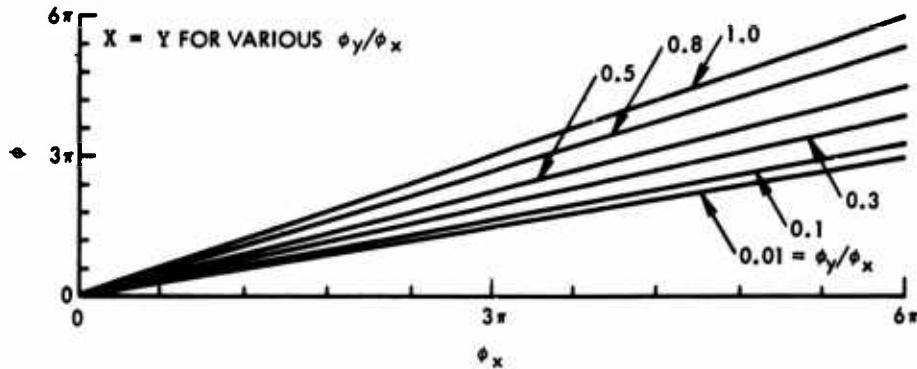


Figure 15. θ for Equal Magnitude Waves Traveling in Same Direction; Effect of θ_y/θ_x

3b. Unequal Magnitude Components

In general, the two traveling waves will have unequal magnitudes. In such a case, certain characteristics of θ can be observed by rewriting equation (9) as

$$\theta = \tan^{-1} \left[\frac{\frac{X}{Y} + \left(\frac{\sin \theta_y}{\sin \theta_x} \right)}{\frac{X}{Y} + \left(\frac{\cos \theta_y}{\cos \theta_x} \right)} \right] \tan \theta_x \quad (22)$$

In the above equation, we assume X to be the dominant component. (This is done arbitrarily for convenience, and Y and θ_y can easily be substituted for X and θ_x , yielding the same results.) For $(X/Y) \gg 1$, this term dominates and $\theta \rightarrow \theta_x$, regardless of the value of (θ_y/θ_x) . For $(\theta_y/\theta_x) < 1$ and $X/Y = O(1)$, the trigonometric terms introduce periodic variations about the line $\theta = \theta_x$. At $X/Y = 1$, of course, equation (21) applies.

In actual computations, in order to get the results of equation (21), it is critical that X/Y be within a fraction of a percent from 1. This is shown

in figures 16 and 17. Clearly, for $(\theta_y/\theta_x) = 1$, $\theta = \theta_x$. For $(\theta_y/\theta_x) > 1$ and $X/Y = 0(1)$, again periodic variations about the line $\theta = \theta_x$ are introduced. However, computationally, if X/Y gets "too close" to 1, jumps of π or 2π may occur. This is shown in figures 18 and 19. Also, the periodicity of these variations is $[1/(1-\theta_y/\theta_x)] 2\pi$. Thus, in figures 16 and 17, the periodicity of the variation about the line $\theta = \theta_x$ is $(10/9)2\pi$ and 4π , respectively. In figures 18 and 19, the periodicity of the variation about the line $\theta = \theta_x$ is -2π and $-\pi$, respectively. The positive or negative sign determines whether the variation is initiated above or below the line $\theta = \theta_x$.

4. Two Waves Traveling in Opposite Directions

The results for two waves traveling in opposite directions are almost the same as in section 3. (p. 10), except for the sign change in θ_y and $\sin \theta_y$. The main difference is in the periodicity of the coherence function and in the periodicity of the variations about the line $\theta = \theta_x$. As mentioned in subsection 3b., the periodicity of these variations is $[1/(1 - \theta_y/\theta_x)] 2\pi$. Therefore, for $(\theta_y/\theta_x) = -0.1$ (see figure 20) and $(\theta_y/\theta_x) = -2$ (see figure 21), these periodicities are $(10/11)2\pi$ and $2\pi/3$, respectively. For comparison purposes one should refer to figures 16 and 18. There the periodicities are $(10/9)2\pi$ and -2π , respectively, where $(\theta_y/\theta_x) = +0.1$ and $+2$.

ADDITIONAL COMMENTS

Unfortunately, similar and, in some cases, identical phase plots arise from completely different combinations of self-noise mechanisms. The same is true for coherence plots. These ambiguities are usually resolved by looking at both the phase and coherence. However, care must be exercised.

As a simple example, one notes that for equal magnitude traveling waves equation (21) shows $\theta = (\theta_x + \theta_y)/2$. Denoting cases 1 and 2 by their respective subscripts, we see that for $\theta_{x1} + \theta_{y1} = \theta_{x2} + \theta_{y2}$ the phase plots are indistinguishable. In terms of wave speed, this becomes

$$d_1 \left(\frac{1}{c_{x1}} + \frac{1}{c_{y1}} \right) = d_2 \left(\frac{1}{c_{x2}} + \frac{1}{c_{y2}} \right).$$

Since the spacing between sensors is known and is the same in both cases, any combination of c_{x1} , c_{y1} and c_{x2} , c_{y2} that satisfies the above yields the same and, therefore, ambiguous result. Consider an investigator who observes a straight line phase plot with a slope of $0.6^\circ/\text{Hz}$ for a sensor spacing of 6 in. He might interpret the result to be a single wave traveling at 300 ft/sec, where $c = 360 \text{ d}/(\theta/f)$. Call this case 1. However, the investigator might not have noticed electronic noise that was combining with a wave equal in magnitude to the electronic noise and traveling at 150 ft/sec. Call this case 2. Then, $c_{x1} = c_{y1} = 300 \text{ ft/sec}$, while $c_{x2} = 150 \text{ ft/sec}$ and $c_{y2} \rightarrow \infty$. Although both cases 1 and 2 yield the same phase plot, they can be easily distinguished by studying the coherence plots. Case 1 shows a constant magnitude coherence, whereas case 2 reflects a periodicity with respect to frequency.

In another example, a wave with $\theta_y = -\theta_x$ is compared with the sum of two waves traveling in the same direction. The wave with $\theta_y = -\theta_x$ has traveling wave components X_{sw} and Y_{sw} and phase θ_{xsw} . The two waves traveling in the same direction have components X_{tw} and Y_{tw} , with phases θ_{xtw} and θ_{ytw} . It was mentioned in section 3. (p. 10) that the magnitude coherences are identical

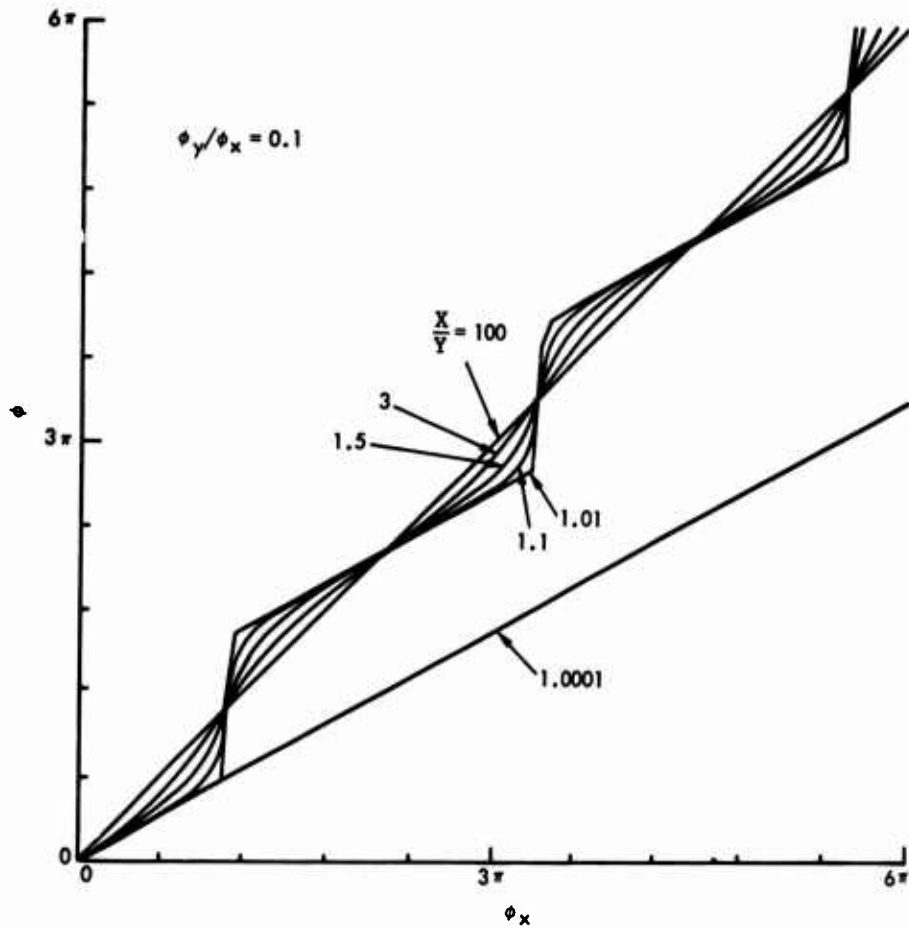


Figure 16. ϕ for Unequal Magnitude Waves Traveling in Same Direction;
Effect of X/Y With $\phi_y/\phi_x = 0.1$

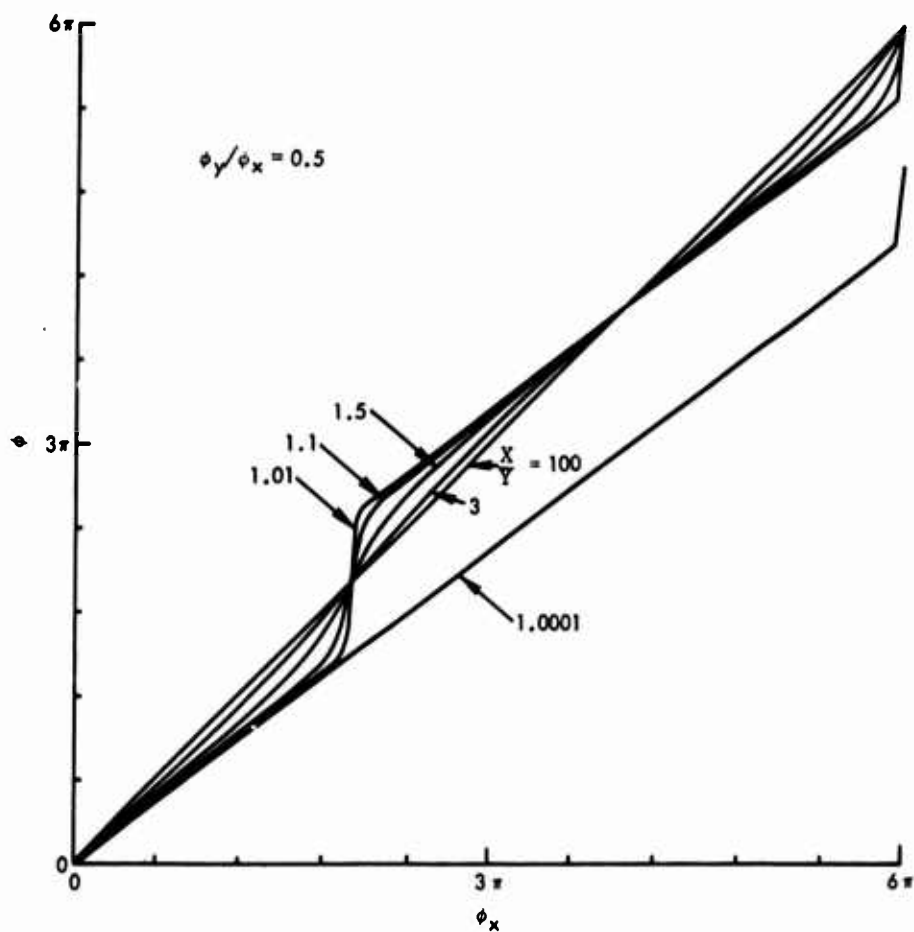


Figure 17. Δ for Unequal Magnitude Waves Traveling in Same Direction;
Effect of X/Y With $\phi_y/\phi_x = 0.5$

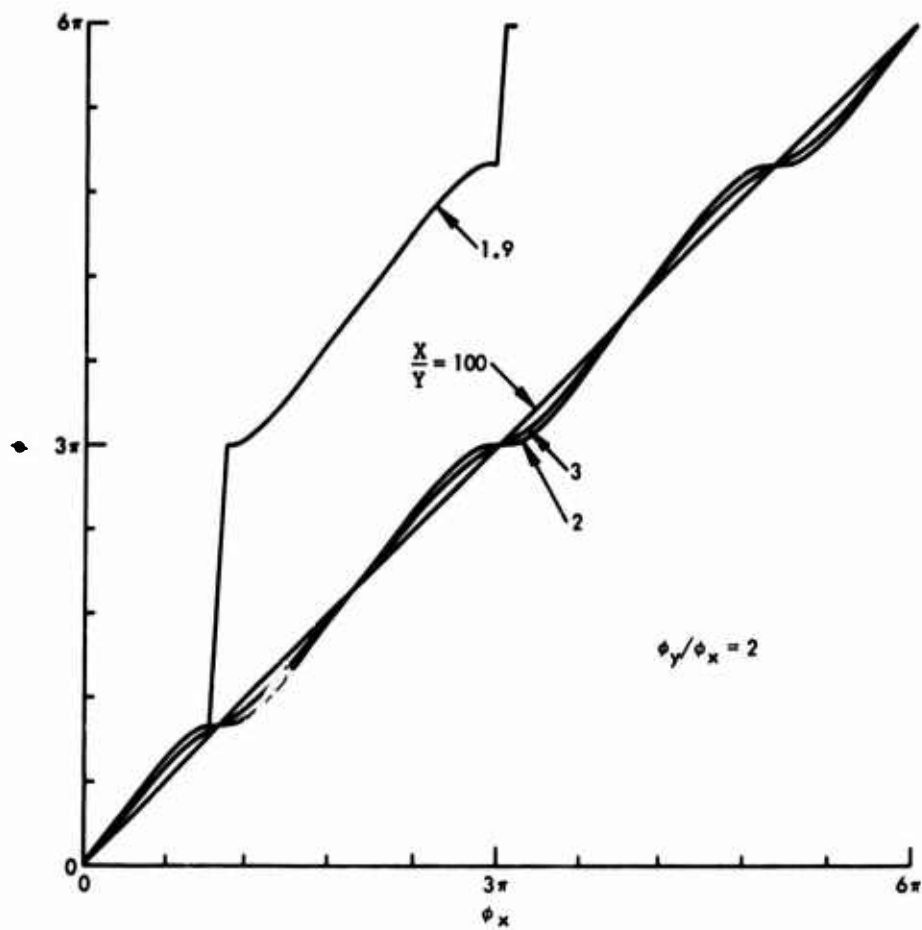


Figure 18. ϕ for Unequal Magnitude Waves Traveling in Same Direction;
Effect of X/Y With $\phi_y/\phi_x = 2$

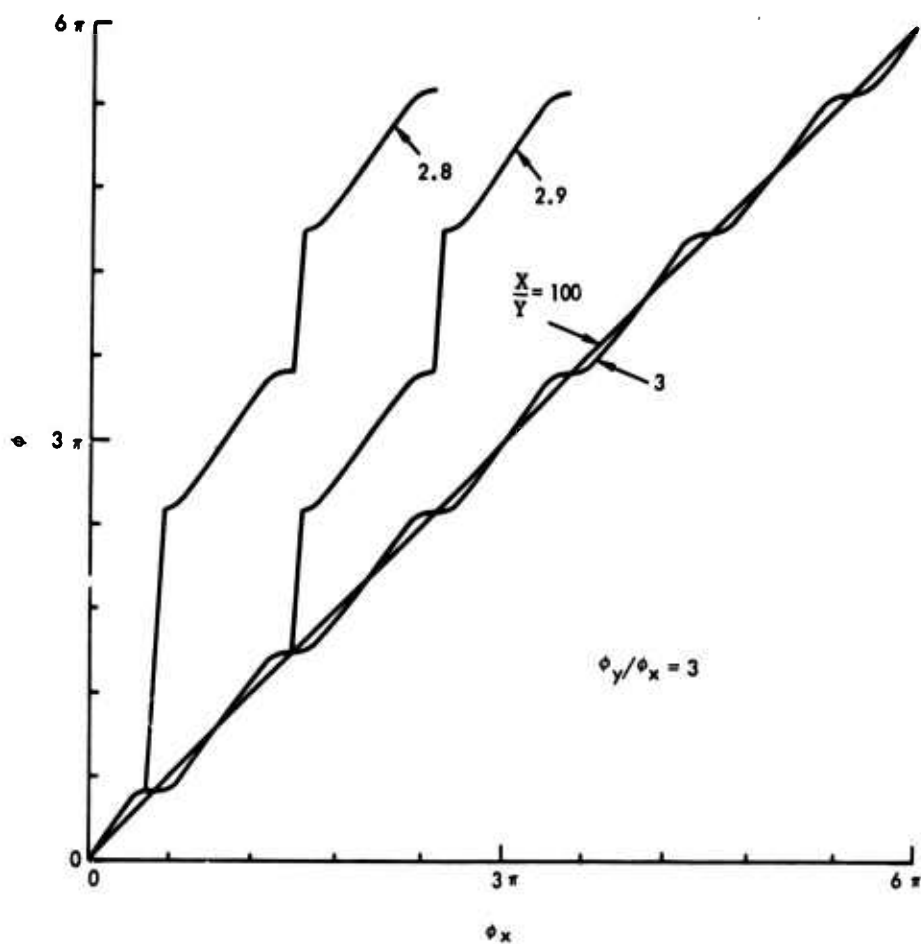


Figure 19. Δ for Unequal Magnitude Waves Traveling in Same Direction;
Effect of X/Y With $\phi_y/\phi_x = 3$

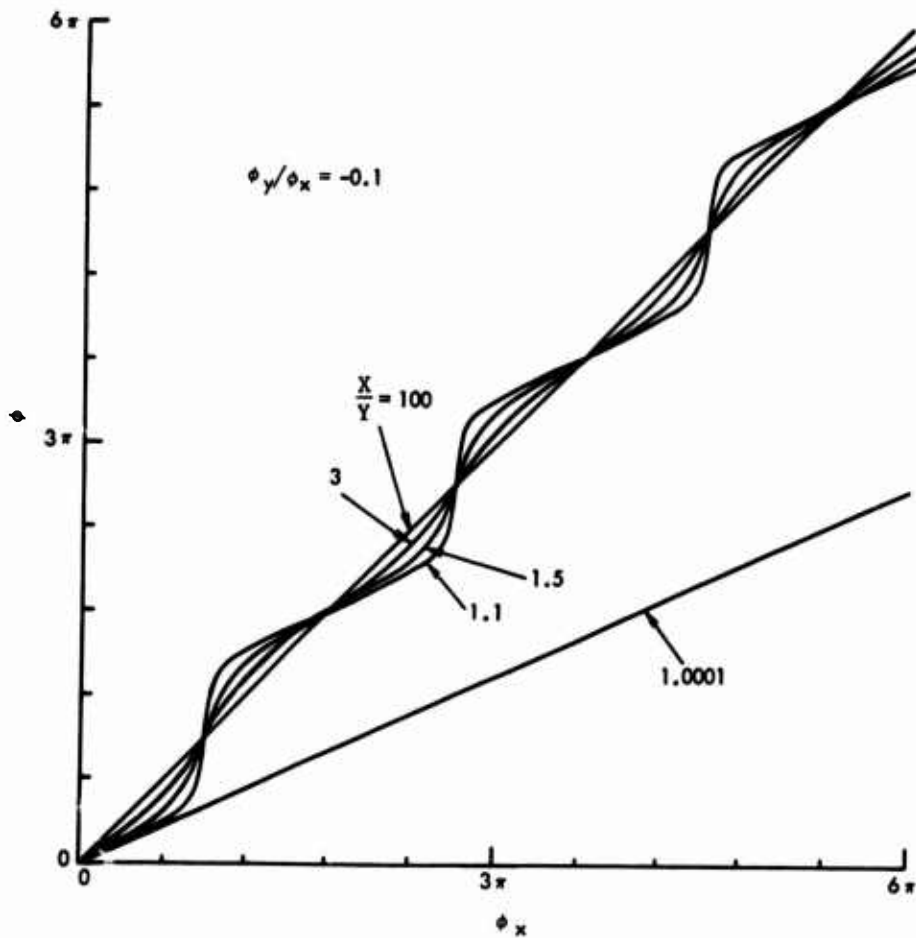


Figure 20. $\Delta\phi$ for Unequal Magnitude Waves Traveling in Opposite Directions; Effect of X/Y With $\phi_y/\phi_x = -0.1$

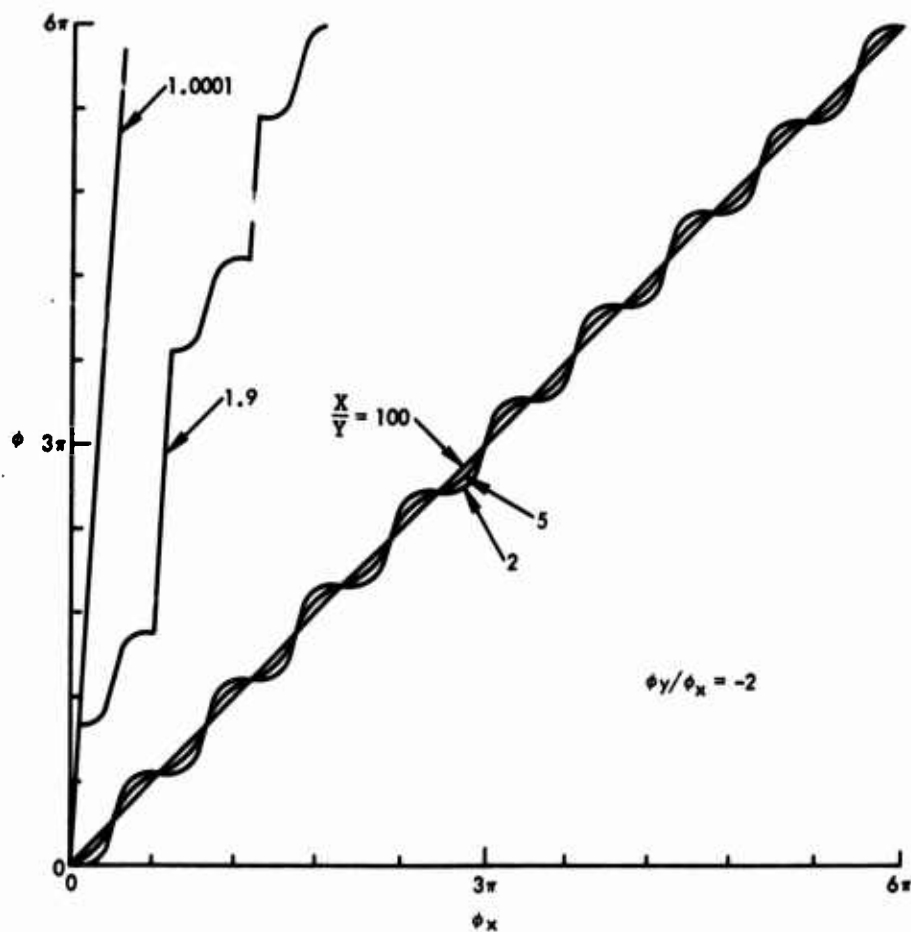


Figure 21. ϕ for Unequal Magnitude Waves Traveling in Opposite Directions; Effect of X/Y With $\phi_y/\phi_x = -2$

if $X_{sw} = X_{tw}$, $Y_{sw} = Y_{tw}$ and $2\theta_{X_{sw}} = (\theta_{xtw} - \theta_{ytw})$. If $c_{xsw} = 300$ ft/sec, $c_{xtw} = 150$ ft/sec, and $c_{ytw} = 5000$ ft/sec, the results are not identical but so close as to render them indistinguishable. The two cases, however, are easily distinguished by noting the phase. A straight line drawn through the periodic variations will determine the speed of the dominant wave (in this case either 300 or 150 ft/sec).

The final example compares two waves, denoted X_s and Y_s , traveling in the same direction with two waves, denoted X_o and Y_o , traveling in opposite directions. Following the convention adopted in subsection 3b. (p. 12), we assume X to be the dominant component. Then, if $X_o = X_s$, $Y_o = Y_s$ and if $c_{Xo} = c_{Xs}$, the only observable difference in both the phase and coherence plots would be in the periodicity with respect to frequency as a result of the fact that $c_{Yo} \neq c_{Ys}$. The observed periodicity, as mentioned previously, is $[1/(1-\theta_y/\theta_x)] 2\pi$ with respect to θ_x . Since, in actual practice, data are obtained as a function of frequency (not θ_x , which is what the investigator is seeking to determine), this periodicity is $\Delta f = \left[\left(\frac{1}{d} \right) \left(\frac{1}{c_x} - \frac{1}{c_y} \right) \right]$ or, denoting $(\theta_y/\theta_x) = (c_x/c_y) = \alpha$,

$$\Delta f = c_x/d(1-\alpha). \quad (23)$$

In order for the periodicities to be the same, Δf_s would have to equal Δf_o , which would require that $\alpha_s = \alpha_o$, since d is the same in both cases, as is c_x (by definition). This is impossible because α_s is always positive and α_o always negative. It is, however, possible to obtain $\Delta f_o = -\Delta f_s$. This would produce an identical periodicity in the coherence plots for both cases. Also, the same periodicity would be produced in the phase plots for both cases, but with a half-period phase shift. This is all shown in figure 22.

It is hoped that the results obtained, along with the examples presented, are of help to those analyzing these types of data. For convenience the results are summarized in table 1.

In actual practice, the reduced data are usually more complicated owing to (1) the presence of more than two self-noise mechanisms, (2) dispersive waves, (3) damping, (4) the statistical dependence of waves as a result of reflections, and (5) the dependence of all pertinent parameters on frequency. If desirable, the investigator can often minimize these complications by careful experiment design.

The investigator should also look at the time domain data, in particular the cross correlation, to shed light on or to confirm his analysis. Periodicities occurring in the frequency domain might be seen more readily via a Cepstrum analysis⁷ or a Smoothed Coherence Transform (SCOT).^{8,9}

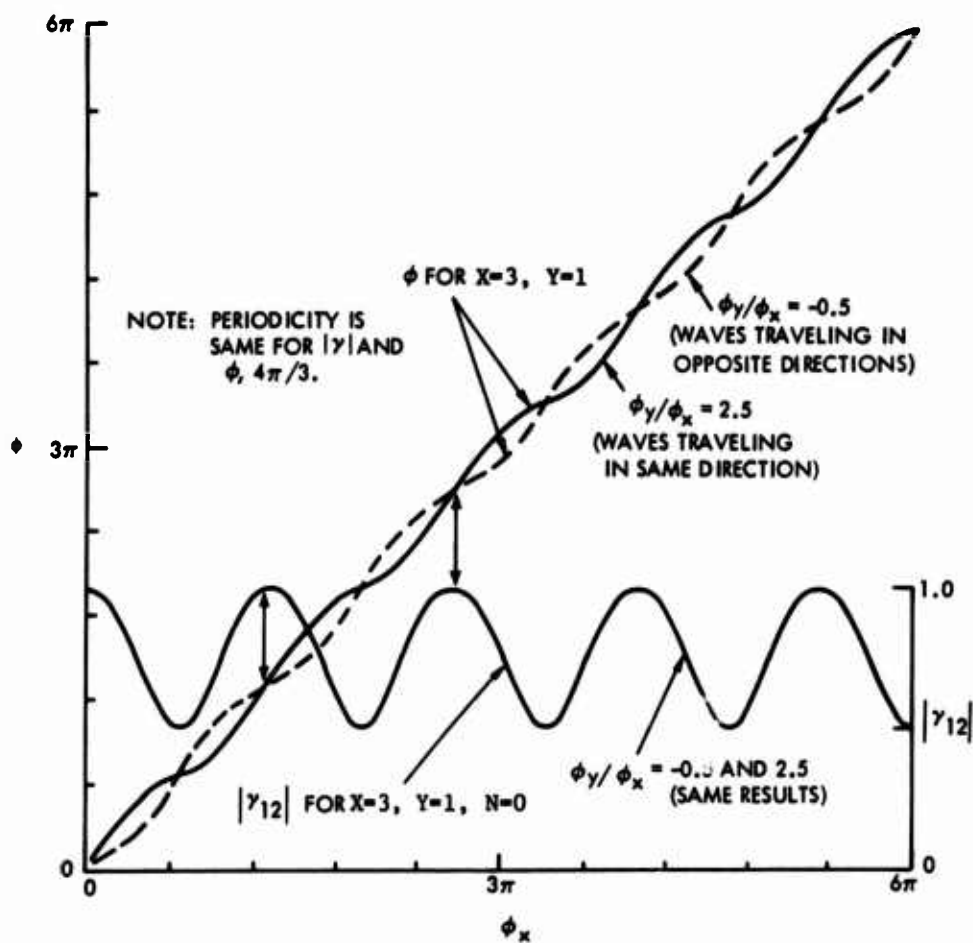


Figure 22. Resolving an Ambiguity

Table 1. Summary of Results

Waveform*	Magnitude Coherence	Phase	Periodicity with Respect to θ_x	Periodicity with Respect to f
1. Single Traveling Wave	$ v_{12} = \frac{X}{X+N}$	$\theta = \theta_x$	∞ (for $ v $ and θ)	∞ (for $ v $ and θ)
2. Waves with $\theta_y = -\theta_x$ a. Equal magnitude traveling wave components (classical standing wave) b. Unequal magnitude traveling wave components	$ v_{12} = \frac{2X}{2X+N} \cos \theta_x$ $ v_{12} = \frac{(X^2 + Y^2 + 2XY \cos 2\theta_x)^{1/2}}{X + Y + N}$	$\theta = \begin{cases} 0 & \tan \theta_x \text{ is positive} \\ \pi & \tan \theta_x \text{ is negative} \end{cases}$ $\theta = \tan^{-1} \left[\frac{X-Y}{X+Y} \tan \theta_x \right]$	∞ (for $ v $ and θ) ∞ (for $ v $ and θ) ∞ (for $ v $ and θ)	$\frac{c_x}{\Delta f} = \frac{2d}{\Delta f}$ (for $ v $ and θ) $\frac{c_x}{\Delta f} = \frac{2d}{\Delta f}$ (for $ v $ and θ)
3. Two waves traveling in same direction a. Equal magnitude components b. Unequal magnitude components	$ v_{12} = \frac{X[2 + 2 \cos(\theta - \theta_y)]^{1/2}}{2X + N}$ $ v_{12} = \frac{[X^2 + Y^2 + 2XY \cos(\theta - \theta_y)]^{1/2}}{X + Y + N}$	$\theta = \frac{\theta_x + \theta_y}{2}$ $\theta = \tan^{-1} \frac{(X \sin \theta_x + Y \sin \theta_y)}{(X \cos \theta_x + Y \cos \theta_y)}$	$2\pi[1/(1 - \theta_y/\theta_x)]$ (for $ v $) ∞ (for θ) $2\pi[1/(1 - \theta_y/\theta_x)]$ (for $ v $ and θ)	$\Delta f = [c_x/d(1-\alpha)]$ $\alpha = (c_x/c_y)$ (for $ v $) (for θ) $\Delta f = [c_x/d(1-\alpha)]$ $\alpha = (c_x/c_y)$ (for $ v $ and θ)
4. Two waves traveling in opposite directions	Same as waveforms 3a. and 3b. where $(\theta_y/\theta_x) < 0$ is understood.			

* Includes uncorrelated noise.

Appendix

DERIVATION OF MAGNITUDE COHERENCE AND PHASE FOR
TWO TRAVELING WAVES IN THE PRESENCE OF UNCORRELATED NOISE

Two traveling waves plus random noise are measured at observation points 1 and 2.* At $\omega = \omega_0$ the observed signals are, respectively,

$$S_1 = n_1 e^{i\omega_0 t + i\theta_{n1}} + X e^{i\omega_0 (t - \frac{x_1}{c_x}) + i\theta_x} + Y e^{i\omega_0 (t - \frac{x_1}{c_y}) + i\theta_y} \quad (A-1)$$

and

$$S_2 = n_2 e^{i\omega_0 t + i\theta_{n2}} + X e^{i\omega_0 (t - \frac{x_2}{c_x}) + i\theta_x} + Y e^{i\omega_0 (t - \frac{x_2}{c_y}) + i\theta_y}, \quad (A-2)$$

where θ_{n1} , θ_{n2} , θ_x , and θ_y are the initial phases associated with a particular observation, and $n_1 = n_1(\omega)$, $n_2 = n_2(\omega)$, $X = X(\omega)$, and $Y = Y(\omega)$ are understood. Also note X is a traveling wave as distinguished from x the spatial coordinate.

The autocorrelation at point 1 is

$$\begin{aligned} R_{11}(\tau) = & \frac{1}{T} \left[\int_{-T/2}^{T/2} n_1^2 e^{i\omega_0 \tau} dt + \int_{-T/2}^{T/2} n_1 X e^{i\omega_0 \tau - i\omega_0 (\frac{x_1}{c_x}) + i(\theta_x - \theta_{n1})} dt \right. \\ & + \int_{-T/2}^{T/2} n_1 Y e^{i\omega_0 \tau - i\omega_0 (\frac{x_1}{c_y}) + i(\theta_y - \theta_{n1})} dt + \int_{-T/2}^{T/2} X^2 e^{i\omega_0 \tau} dt \\ & + \int_{-T/2}^{T/2} X n_1 e^{i\omega_0 \tau + i\omega_0 (\frac{x_1}{c_x}) + i(\theta_{n1} - \theta_x)} dt + \int_{-T/2}^{T/2} X Y e^{i\omega_0 \tau + i\omega_0 (\frac{x_1}{c_x} - \frac{x_1}{c_y}) + i(\theta_y - \theta_x)} dt \\ & + \int_{-T/2}^{T/2} Y n_1 e^{i\omega_0 \tau + i\omega_0 (\frac{x_1}{c_y}) + i(\theta_{n1} - \theta_y)} dt + \int_{-T/2}^{T/2} Y X e^{i\omega_0 \tau + i\omega_0 (\frac{x_1}{c_y} - \frac{x_1}{c_x}) + i(\theta_x - \theta_y)} dt \\ & \left. + \int_{-T/2}^{T/2} Y^2 e^{i\omega_0 \tau} dt \right] . \quad (A-3) \end{aligned}$$

*The approach taken in this appendix was suggested by Dr. A. H. Nuttall, of NUSC.

The corresponding autospectrum is

$$\begin{aligned}
 G_{11}(\omega) = & (N_1^2 + X^2 + Y^2) 2\pi\delta(\omega-\omega_0) \\
 & + n_1 X \left[e^{-i\omega_0 x_1/c_x} e^{i(\theta_x - \theta_{n1})} + e^{i\omega_0 x_1/c_x} e^{i(\theta_{n1} - \theta_x)} \right] 2\pi\delta(\omega-\omega_0) \\
 & + n_1 Y \left[e^{-i\omega_0 x_1/c_y} e^{i(\theta_y - \theta_{n1})} + e^{i\omega_0 x_1/c_y} e^{i(\theta_{n1} - \theta_y)} \right] 2\pi\delta(\omega-\omega_0) \\
 & + XY \left[e^{i\omega_0 \left(\frac{x_1}{c_x} - \frac{x_1}{c_y} \right)} e^{i(\theta_y - \theta_x)} + e^{i\omega_0 \left(\frac{x_1}{c_y} - \frac{x_1}{c_x} \right)} e^{i(\theta_x - \theta_y)} \right] 2\pi\delta(\omega-\omega_0). \quad (A-4)
 \end{aligned}$$

Taking θ_{n1} , θ_{n2} , θ_x , and θ_y as uniformly distributed random variables and ensemble averaging, we get

$$\hat{G}_{11}(\omega) = (n_1^2 + X^2 + Y^2) 2\pi\delta(\omega-\omega_0). \quad (A-5)$$

All cross terms involving differences between initial phase angles go to zero. This can be seen as follows:

$$\overline{e^{i(\theta_b - \theta_a)}} = \int_{-\pi}^{\pi} \int_{-\pi}^{\pi} e^{i(\theta_b - \theta_a)} P(\theta_b) P(\theta_a) d\theta_b d\theta_a, \quad (A-6)$$

where $P(\theta_b, \theta_a) = P(\theta_b)P(\theta_a)$ for statistical independence.

$$\text{Taking } P(\theta_a) = \frac{1}{2\pi} \begin{cases} -\pi \leq \theta_a \leq \pi \\ 0 \end{cases} \text{ and } P(\theta_b) = \frac{1}{2\pi} \begin{cases} -\pi \leq \theta_b \leq \pi \\ 0 \end{cases},$$

we get

$$\overline{e^{i(\theta_b - \theta_a)}} = \frac{1}{4\pi} \int_{-\pi}^{\pi} \int_{-\pi}^{\pi} e^{i(\theta_b - \theta_a)} d\theta_b d\theta_a = 0. \quad (A-7)$$

Therefore, $P(\theta_a)$ or $P(\theta_b)$ must be uniformly distributed to have the cross terms drop out.

Similarly one obtains

$$\hat{G}_{22}(\omega) = (n_2^2 + X^2 + Y^2) 2\pi\delta(\omega-\omega_0). \quad (A-8)$$

Writing the cross correlation and ensemble averaging yields the cross spectrum $\hat{G}_{12}(\omega)$:

$$\hat{G}_{12}(\omega) = \left[X^2 e^{i\omega_0 \left(\frac{x_1 - x_2}{c_x} \right)} + Y^2 e^{i\omega_0 \left(\frac{x_1 - x_2}{c_y} \right)} \right] 2\pi \delta(\omega - \omega_0), \quad (\text{A-9})$$

and the coherence is simply

$$\gamma_{12} = \frac{X^2 e^{i\omega_0 \left(\frac{x_1 - x_2}{c_x} \right)} + Y^2 e^{i\omega_0 \left(\frac{x_1 - x_2}{c_y} \right)}}{\left[(n_1^2 + X^2 + Y^2) (n_2^2 + X^2 + Y^2) \right]^{1/2}}. \quad (\text{A-10})$$

This is identical to equation (3), where

$$X^2(\omega) = X(f), \quad Y^2(\omega) = Y(f), \quad \text{and} \quad n_1(\omega)^2 = n_2(\omega)^2 = N(f).$$

Also, $(x_1 - x_2) = d$.

When θ_x and θ_y have deterministic relationships, different results are effected. Consider, for example, when $\theta_x = \theta_y = 0$, the observed signals are

$$S_1 = n_1 e^{i\omega_0 t} + X e^{i\omega_0 \left(t - \frac{x_1}{c_x} \right)} + Y e^{i\omega_0 \left(t - \frac{x_1}{c_y} \right)} \quad (\text{A-11})$$

and

$$S_2 = n_2 e^{i\omega_0 t} + X e^{i\omega_0 \left(t - \frac{x_1}{c_x} \right)} + Y e^{i\omega_0 \left(t - \frac{x_2}{c_y} \right)}. \quad (\text{A-12})$$

Note, only X and Y are not independent; however, n_1 and n_2 are independent relative to each other and to X and Y . Since, as observed previously, all cross terms involving n_1 and n_2 will drop out after ensemble averaging, there is no need to demonstrate this further by incorporating the initial phase angles. Also, $n_1 = n_1(\omega)$, $n_2 = n_2(\omega)$, $X = X(\omega)$, and $Y = Y(\omega)$ is understood.

The autocorrelation at point 1 is

$$R_{11}(\tau) = \frac{1}{T} \left[\int_{-T/2}^{T/2} n_1 n_1 e^{i\omega_0 \tau} dt + \int_{-T/2}^{T/2} X^2 e^{i\omega_0 \tau} dt + \int_{-T/2}^{T/2} Y^2 e^{i\omega_0 \tau} dt \right. \\ \left. + \int_{-T/2}^{T/2} X Y e^{i\omega_0 \tau} e^{i\omega_0 \left(\frac{x_1}{c_x} - \frac{x_1}{c_y} \right)} dt + \int_{-T/2}^{T/2} Y X e^{i\omega_0 \tau} e^{i\omega_0 \left(\frac{x_1}{c_y} - \frac{x_1}{c_x} \right)} dt \right] \quad (\text{A-13})$$

and

$$\hat{G}_{11}(\omega) = n_1^2 2\pi\delta(\omega - \omega_0) + (X^2 + Y^2)2\pi\delta(\omega - \omega_0) + XY \left[e^{i\omega_0 \left(\frac{x_1}{c_x} - \frac{x_1}{c_y} \right)} + e^{i\omega_0 \left(\frac{x_1}{c_y} - \frac{x_1}{c_x} \right)} \right] 2\pi\delta(\omega - \omega_0) \quad (A-14)$$

Similarly,

$$\hat{G}_{22}(\omega) = n_2^2 2\pi\delta(\omega - \omega_0) + (X^2 + Y^2)2\pi\delta(\omega - \omega_0) + XY \left[e^{i\omega_0 \left(\frac{x_2}{c_x} - \frac{x_2}{c_y} \right)} + e^{i\omega_0 \left(\frac{x_2}{c_y} - \frac{x_2}{c_x} \right)} \right] 2\pi\delta(\omega - \omega_0) \quad (A-15)$$

The cross spectrum is readily obtained:

$$\hat{G}_{12}(\omega) = \left\{ X^2 e^{i\omega_0 \left(\frac{x_1}{c_x} - \frac{x_2}{c_x} \right)} + Y^2 e^{i\omega_0 \left(\frac{x_1}{c_y} - \frac{x_2}{c_y} \right)} + XY \left[e^{i\omega_0 \left(\frac{x_1}{c_x} - \frac{x_2}{c_y} \right)} + e^{i\omega_0 \left(\frac{x_1}{c_y} - \frac{x_2}{c_x} \right)} \right] \right\} 2\pi\delta(\omega - \omega_0) \quad (A-16)$$

Also, one may write

$$\hat{G}_{11}(\omega) = n_1^2 2\pi\delta(\omega - \omega_0) + \left| X e^{-i\omega_0 \frac{x_1}{c_x}} + Y e^{-i\omega_0 \frac{x_1}{c_y}} \right|^2 2\pi\delta(\omega - \omega_0), \quad (A-17)$$

$$\hat{G}_{22}(\omega) = n_2^2 2\pi\delta(\omega - \omega_0) + \left| X e^{-i\omega_0 \frac{x_2}{c_x}} + Y e^{-i\omega_0 \frac{x_2}{c_y}} \right|^2 2\pi\delta(\omega - \omega_0), \quad (A-18)$$

$$\hat{G}_{12}(\omega) = \left[X e^{i\omega_0 \frac{x_1}{c_x}} + Y e^{i\omega_0 \frac{x_1}{c_y}} \right] \left[X e^{-i\omega_0 \frac{x_2}{c_x}} + Y e^{-i\omega_0 \frac{x_2}{c_y}} \right] 2\pi\delta(\omega - \omega_0) \quad (A-19)$$

and, ignoring uncorrelated noise sources, as was done previously in equation (6),

$$\hat{G}_{12}(\omega) = \frac{\left(X e^{+i\omega_0 x_1/c_x} + Y e^{+i\omega_0 x_1/c_y} \right) \left(X e^{-i\omega_0 x_2/c_x} + Y e^{-i\omega_0 x_2/c_y} \right)}{\left| X e^{-i\omega_0 x_1/c_x} + Y e^{-i\omega_0 x_1/c_y} \right|^2 \left| X e^{-i\omega_0 x_2/c_x} + Y e^{-i\omega_0 x_2/c_y} \right|^2} \quad (A-20)$$

Finally, one notes that for a standing wave, $c_x = -c_y = c$ and equation (A-20) becomes

$$\hat{C}_{12}(\omega) = \frac{\left(X e^{+i\omega_0 x_1/c} + Y e^{-i\omega_0 x_1/c} \right) \left(X e^{-i\omega_0 x_2/c} + Y e^{+i\omega_0 x_2/c} \right)}{\left| X e^{-i\omega_0 x_1/c} + Y e^{+i\omega_0 x_1/c} \right|^2 \left| X e^{-i\omega_0 x_2/c} + Y e^{+i\omega_0 x_2/c} \right|^2}; \quad (\text{A-21})$$

for $X = Y$,

$$\left| \gamma_{12}(\omega) \right| = \left| \frac{\cos \omega_0(x_1/c) \cos \omega_0(x_2/c)}{\cos \omega_0 x_1/c \cos \omega_0 x_2/c} \right|, \quad (\text{A-22})$$

which is identical to equation (6).

LIST OF REFERENCES

1. NUSC letter to Commander, Naval Ship Systems Command Headquarters, "STAMM Cross Spectral Analysis of At-Sea Data," ser. SA14-114, 29 March 1974.
2. A. E. Markowitz, "The Effects of Spiky Events Occurring Simultaneously on All Channels of Recorded Data," NUSC Technical Memorandum SA14-210-74, 31 July 1974.
3. A. E. Markowitz, "Data Report on Second At-Sea STAMM Test - April 1974," NUSC Data Report SA14-21F-74, 22 October 1974.
4. G. C. Carter, C. H. Knapp, and A. H. Nuttall, "Estimation of the Magnitude Squared Coherence Function Via Overlapped FFT Processing," IEEE Transactions on Audio and Electroacoustics, vol. AU-21, no. 4, August 1973, pp. 337-344.
5. Binary Systems, Inc., letter to Commander, NUSC, ser. B74-873, 11 June 1974.
6. NUSC letter to Binary Systems, Inc., "Comments on the Coherence Function as Seen in the Excised STAMM Data," ser. SA14-227, 16 August 1974.
7. A. M. Knoll, "The Cepstrum and Some Close Relatives," Proceedings of the NATO Advanced Study Institute on Signal Processing, Academic Press, New York, 1973.
8. G. C. Carter, A. H. Nuttall, and P. G. Cable, "The Smoothed Coherence Transform," Proceedings of the IEEE, vol. 31, no. 10, October 1973, pp. 1497-8.
9. G. C. Carter and C. H. Knapp, "Coherence and Its Estimation via the Partitioned Modified Chirp-Z Transform," IEEE Transactions on Acoustics, Speech, and Signal Processing, vol. ASSP-23, no. 3, June 1975, pp. 257-264.